PERGAMON

Journal of Structural Geology 21 (1999) 1189–1197

JOURNAL OF STRUCTURAL GEOLOGY

www.elsevier.nl/locate/jstrugeo

How pressure solution creep and fracturing processes interact in the upper crust to make it behave in both a brittle and viscous manner

Jean-Pierre Gratier*, François Renard, Pierre Labaume

LGIT, CNRS-Observatoire, Université Joseph Fourier, IRIGM, BP 53X, 38041 Grenoble, France

Received 12 February 1998; accepted 4 January 1999

Abstract

The upper crust has been described as being dominated by brittle deformation along faults, or ductile where folds and cleavage have developed. These two mechanical behaviors are explained by two different mechanisms of deformation: (i) fracture; and (ii) fluid-enhanced deformation (e.g. pressure solution). These two mechanisms operate at two time scales: fast for brittle deformation, slow for pressure solution. Natural observations of relationships between pressure solution and fractures in sandstones, or indented pebbles, and experimental results of pressure solution with an indenter technique indicate that both mechanisms can interact: fracture development increases the kinetics of the pressure solution process, pressure solution relaxes the stress between fracturing events. A simple model of brittle–ductile deformation, applied to indented limestone pebbles, shows that cycles of slow deformation can alternate with short-time fracture.

1. Introduction

Earthquakes and fractures which occur in the upper crust testify to its brittle behavior. However, natural structures such as folds and cleavage, which also develop in the entire upper crust, are evidence for a ductile and viscous behavior. Laboratory experiments partially explain this paradox by showing that the two types of behavior do not occur over the same time scale: dynamic fracturing is favored over very short time scales, and viscous dissolution precipitation creep proceeds over much longer time scales. However, these two deformation mechanisms are very often spatially associated in the upper crust (Onasch, 1990; Onasch and Dunne, 1993). Therefore, it is crucial to understand how these two processes interact in order to gain an improved insight into the complex mechanical behavior of the upper crust (De Bremaecker, 1987; Gratier and Gamond, 1990; Shen et al., 1997).

Subcritical crack growth may act over intermediate time scales (Atkinson, 1984; Darot et al., 1985); however, the slowest experimental crack propagation values (10^{-8} m s^{-1}) seem to indicate that such a mechanism is relatively fast vs pressure solution strain-rate (see below).

Examples of interactions between fractures and pressure solution are briefly presented both from indentation experiments and from natural deformation in limestone pebbles in a conglomerate and quartz grains in a sandstone. Thus a new model is proposed which integrates both the evolution of the geometry of deformed blocks (grains, pebbles) and the interaction between fractures and pressure solution. It is suggested that mechanical modeling of the upper crust (creep laws) must integrate these complex mechano-chemical interactions both by developing new modeling concepts and by acquiring more pertinent experimental data.

2. Experimental approach

The principle of the indenter technique is shown in

* Corresponding author..
E-mail address: gratier@obs.ujf-grenoble.fr (J.P. Gratier)

0191-8141/99/$ - see front matter
PII: S0191-8141(99)00035-8

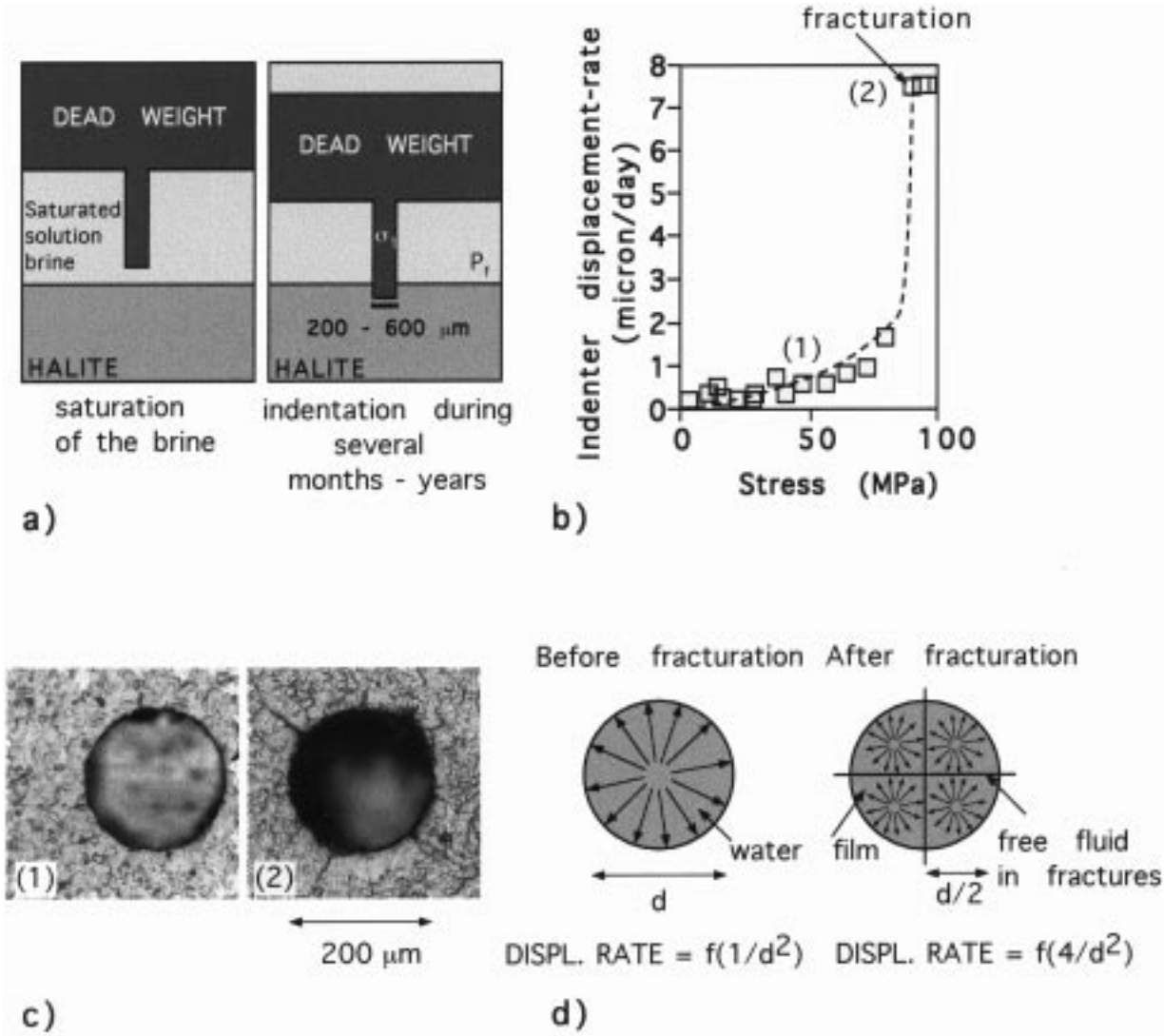

Fig. 1. Experimental results obtained by the indenter technique. (a) Schematic view of experimental device. A cylindrical stainless steel indenter, mounted under a free moving Teflon piston and loaded by a dead weight, is kept in contact with a crystal of halite, in the presence of its brine during several months or years. (b) Experimental rates of indentation for crystals of halite: (1) without any fracture in halite; (2) with fracturing development which increased the rates of indentation. (c) Holes under the indenter: (1) without any fracture on the left (part 1 of curve b); (2) with radial fractures on the right (part 2 of curve b). (d) Fractures develop channels with high diffusion (within free fluid) decreasing the path length for slow diffusion under the indenter (radial arrows along solid–trapped fluid–solid interface) and accelerating the rate of indentation.

Fig. 1(a) (Gratier, 1993a): a cylindrical stainless steel indenter, mounted under a free moving Teflon piston and loaded by a dead weight, is kept in contact with a crystal of halite, in presence of its brine. Before the indenter is put in contact with the sample, the crystal is immersed in the brine already saturated with halite powder, in order to trap a saturated fluid phase under the indenter. Such devices are maintained within a furnace at constant temperature. After long duration experiments (several months, or years) cylindrical holes are formed by dissolution under stress (Gratier, 1993a,b): mass transfer occurs by diffusion along the indenter–trapped fluid–crystal interface, from the area with the highest chemical potential (stressed interface under the indenter) to the area with the lowest chemical potential (free-surface of the crystal). This indenter technique maintains a constant interface area and geometry. The effect of various parameters may be properly tested such as stress, indenter diameter, temperature, nature of the solid and the solution, and other parameters which are presumed to play a crucial role in pressure solution creep laws (cf. creep laws proposed by Weyl, 1959; Raj and Ashby, 1971; Rutter, 1976; Raj, 1982).

Such experiments also show how the development of fractures accelerates the pressure solution process, with only this aspect being presented here. The displacement-rate of the indenter is found to be limited by the slow diffusive mass transfer out of the indenter/trapped fluid/crystal interface. This is shown by the

fact that the displacement rate is inversely proportional to the diameter of the indenter (Gratier, 1993a). A displacement rate vs stress relation is observed (Fig. 1b) which is clearly non-linear as predicted by theoretical approaches (Lehner and Bataille, 1985; Ortoleva, 1994) but this aspect will not be discussed here. Above a yield stress value (90 MPa in Fig. 1b), the displacement rate is drastically increased; this behavior is systematically associated with the development of radial fractures under the indenter (Fig. 1c, hole on the right). The fast displacement rates plotted on Fig. 1(b), for stress values above 90 MPa, are minimum values since the indenters were found blocked at their maximum possible displacement (the length of these indenters). The width of the radial fractures remains very low from the top to the bottom, and is approximately several microns. No deformation or dissolution, within or around these fractures, can explain the increase of the displacement rate. No evidence of plastic deformation is found. Plastic deformation should appear either by the development of a moat of dissolution around the indenter as observed by Tada and Siever (1986) and Gratier (1993a, when using undersaturated solution) or by upswelling of the crystal around the hole to account for constant volume accommodation of plastic flow. Explanations of such a drastic increase of dissolution rate are more likely to be linked to the change of path length of mass transfer induced by fracturing.

At low stress (below 90 MPa), the slow diffusive process along the trapped fluid, which is the limiting process, occurs through the whole diameter of the indenter (Fig. 1d, left part). In this case, using the stress vs displacement-rate relation given in Fig. 1(b), the total product $D \times w$ ($m^3 s^{-1}$) may be estimated, where D is the diffusion coefficient of aqueous species under the indenter and w the thickness of the trapped fluid film. This value is about $2 \times 10^{-19} m^3 s^{-1}$ at 25°C (Gratier, 1993a,b).

At high stress (above 90 MPa), the development of radial fractures, the length of which being larger than the diameter of the indenter, open the possibility of fast mass transfer out of the indenter contact since this transfer occurs within the free fluid which fills the fractures. In this case the product of the diffusion coefficient ($2 \times 10^{-9} m^2 s^{-1}$, see Applin, 1987) and the width of the path of mass transfer (2×10^{-6} m measured on the sample) may be estimated to be $4 \times 10^{-15} m^3 s^{-1}$. Consequently, the initial interface with a slow diffusive path ($2 \times 10^{-19} m^3 s^{-1}$) is partitioned into several small areas with the same slow diffusive paths, separated by channels with fast diffusive paths ($4 \times 10^{-15} m^3 s^{-1}$). The displacement rate of the indenter is limited by the slow diffusive mass transfer out of the slow diffusive interface domains. As the displacement rate is inversely proportional to the square of the distance of mass transfer out of these slow diffusive interfaces (Gratier, 1993a) this displacement rate is drastically increased by the development of the fractures. In this case the displacement rate is inversely proportional to the mean diameter of the slow diffusive interface and not to the whole diameter of the indenter. For example, when a set of two perpendicular fractures divides the initial diameter of the area with slow diffusive path by two, the displacement rate is multiplied by four (Fig. 1d, right part).

A significant increase of pressure solution rate has been assumed to be associated with subcritical microcrack growth during pressure solution as determined from natural and experimental observations, respectively (Gratz, 1991; den Brok, 1998). The main difference with our model is that in the so-called Gratz's model, microcracks develop at the grain boundary scale. Channels are located where finely spaced microcracks intersect the boundary. These channels continuously change position in a dynamic channel-island grain boundary model. Consequently, in the Gratz's model, the microcrack effect is integrated in a stable pressure solution process (as perhaps, the observed behavior below 90 MPa).

3. Natural observations

Observations of natural structures, such as pitted pebbles in compressional basins, or quartz grains in sandstones (Onasch, 1993; Milliken, 1994), show as well the crucial effect of the development of fractures to promote and activate pressure solution. Indented pebbles have been recognized for a long time (Sorby, 1865; McEwen, 1978). Figure 2(a) shows a limestone pebble from Miocene conglomerate near Grenoble (France) where indentation by another pebble has occurred on the top. At the contact, stylolites indicate the presence of dissolution. The geometry of radial fractures around the dissolution interfaces indicates that fractures develop during the dissolution process (McEwen, 1978). These fractures are sealed with calcite. The burial depth of this pebble is estimated to be less than 2 km and the total tectonic deformation (by horizontal shortening) encountered by the pebble has not lasted more than a few million years (Gratier and Gamond, 1990).

Fig. 2(b) and (c) shows microphotographs of Miocene sandstone from the sub-andean zone of southern Bolivia (Moretti et al., 1996). The sandstone is coarse grained (grain size up to 0.3–0.4 mm), highly porous (15–20%) and uncemented. Quartz grains are the most abundant lithology and show typical roundness of original detritial grains. Quartz grains show mainly point contacts, but grain indentation along concavo–convex contacts (Tucker, 1981) are also frequent. There is no visible microbrecciation or plastic

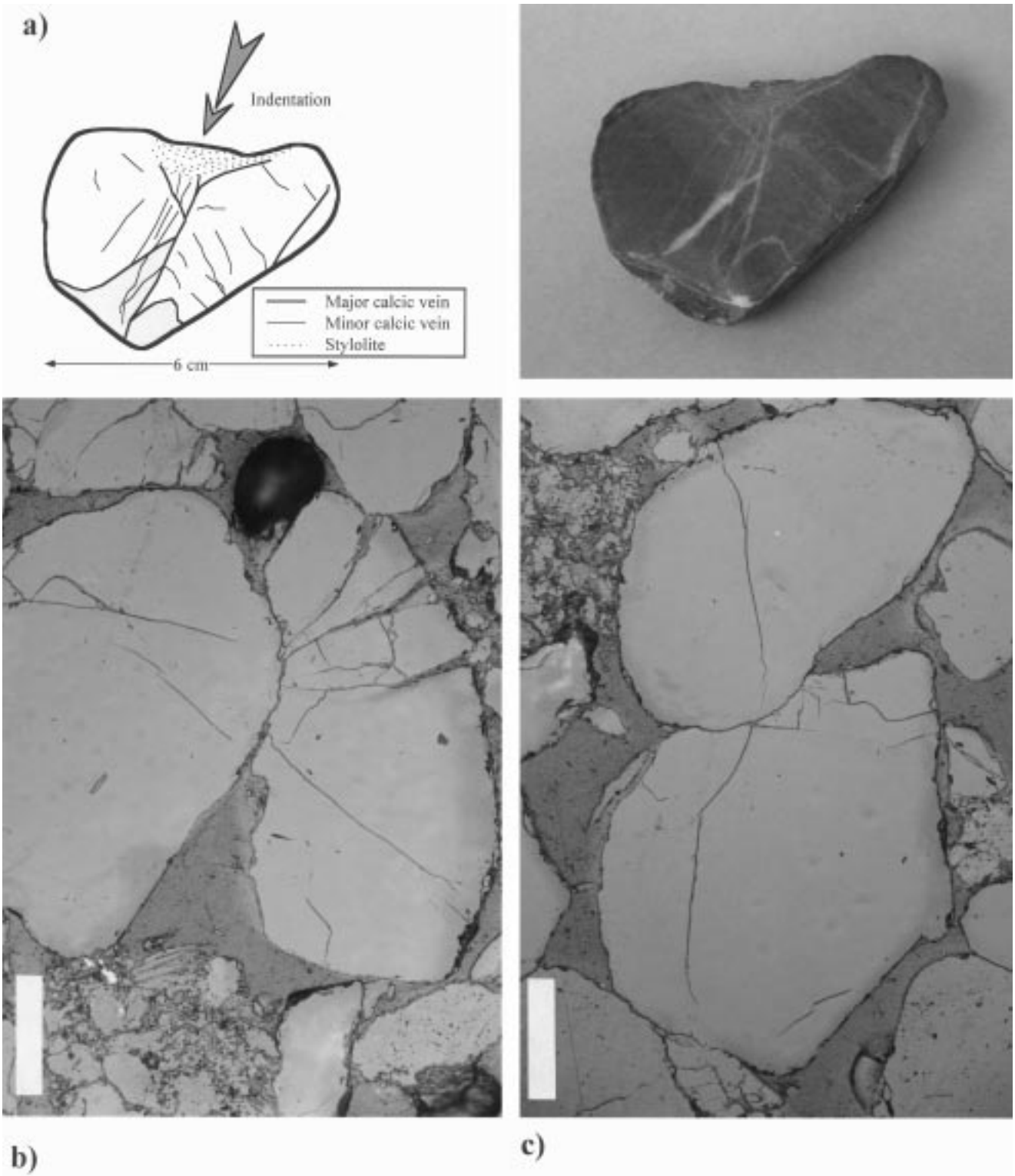

Fig. 2. Natural examples of ductile–fragile interactions. (a) Photograph (right) and schematic representation (left) of a cross-section in a limestone pebble from the Miocene of the area of Grenoble (France). On the dissolution surface area, the stress reached values higher than the yield strength of the pebble and fractures (now calcic veins) have occurred. (b–c) Miocene sandstone from the sub-andean zone of southern Bolivia showing (i) quartz grain indentation along concavo–convex contacts, resulting from pressure solution; and (ii) intragranular extensional fractures originating at indented contacts; microphotographs in reflected light. The large light gray grains are quartz. Dark gray between grains is epoxy resin filling porosity. Scale bar = 0.1 mm.

deformation (no undulose extinction) associated with the indentation contacts. Therefore, grain indentation is thought to result from pressure solution at grain contacts (Houseknecht, 1988). The indented grains show frequently one or several intragranular fracture(s) which originate(s) at the contact zone. Although their detailed geometry may be complex, the fractures are at high angle to the contact and their overall geometry is linear or smoothly curved. They cross the entire grain or nearly so. These geometries suggest that they are extensional (mode I) fractures. They are not sealed or healed, and may show opening of a few microns. The geometrical relationships of the grain indentation and intragranular fractures show that both types of structures were formed in a similar stress regime with shortening sub-perpendicular to the indented grain contacts and sub-parallel to the fractures. At the scale of the thin section, the shortening direction is sub-perpendicular to bedding, i.e. it corresponds to burial compaction. According to the geological context (Moretti et al., 1996), the sediment was submitted successively to: (1) sedimentary burial in the foreland basin (probably <1000 m for the sample shown); (2) tectonic burial under a thrust sheet (probably up to 3000 m); and (3) uplift and erosion. The whole cycle occurred during the Mio-Pliocene. The lack of fracture sealing and of diagenetic quartz overgrowth at the periphery of the grains suggests that the quartz dissolved at grain contacts was drained, i.e. the pressure-solution process took place in an open hydrologic system.

4. Modeling pressure solution interaction with fractures

A creep law for pressure solution has the form:

$$\dot{\varepsilon} = \sigma/\eta \tag{1}$$

where $\dot{\varepsilon}$ is strain rate (s^{-1}), σ is the difference between the normal stress acting on the interface of dissolution and the normal stress acting on the surface of deposition (often assumed to be equal to the pore fluid pressure), η is a viscosity coefficient. A linear stress vs strain-rate relation is used for simplification.

According to Raj and Ashby (1971), Rutter (1976), and Raj (1982), this viscosity coefficient is a function of various parameters and the relation may be expressed as:

$$\dot{\varepsilon} = [\alpha\sigma DwcV]/[RTd^3] \tag{2}$$

where α is a numerical coefficient, D is the diffusion coefficient for the rate limiting species, w is the width of the transport path in the zone of dissolution, c is the solubility of the solid in solution, R is the gas constant, T is the temperature, V is the molar volume of the solid, and d is the grain diameter (assumed to be both the diameter of the surface of dissolution and the size of the closed system for mass transfer).

Constant displacement rate ($m\ s^{-1}$) may be assumed for the modeling of tectonic deformation. This assumption is not appropriate for the compaction process where pressure solution–fracture interaction is probably associated with the progressive increase of stress with depth. For simplicity, only constant displacement rate assumption has been tested in this preliminary study. Assuming such a constant displacement rate between two grains or pebbles as a boundary condition, the evolution of stress with time may be estimated for the case of fractures developing during progressive indentation by pressure solution (Fig. 3a). When considering pressure solution of grains, or pebbles, or any porous (or fractured) aggregate, porosity reduction during the progressive deformation is associated with an increase in the surface of dissolution. Taking into account the stress vs diameter of dissolution ratio (σ/d^2), and without any fracture, the stress value must increase during such a progressive deformation in order to keep the displacement rate constant (stage 1 to 2, Fig. 3a). However, increase of the stress value cannot be infinite since the grains, or pebbles, will necessarily fracture. When stress value reaches the fracture strength of the grains or pebbles (stage 3, Fig. 3a), fractures occur which partition the surface of dissolution into several smaller parts. A new cycle develops (stage 3 to 5, Fig. 3a). According to the indenter experimental results (Fig. 1b, c and d), this fracturing process develops fast diffusive paths of mass transfer and reduces the mean distance of slow diffusive mass transfer (d) along the surface of dissolution. Consequently, the stress value which is needed to maintain constant displacement rate is reduced. An unstable viscous process is predicted which is periodically activated by fracture development.

This model assumes that pressure solution and fracture interactions can be applied to the limestone pebbles of Fig. 2(a). The surface of contact between two spherical limestone pebbles deforms by a three-step pressure solution mechanism: (1) dissolution occurs inside the contact between the two pebbles where stress is high; (2) matter diffuses along the interface, inside a fluid film (Renard and Ortoleva, 1997) to the pore space where (3) it can precipitate. The deformation rate $\dot{\varepsilon}$ (s^{-1}) is related to the rate of indentation G_{ind} ($m\ s^{-1}$) through

$$\dot{\varepsilon} = \frac{G_{ind}}{d} \tag{3}$$

where d is the size of the pebble (Fig. 3a).

It is assumed that diffusion is the slowest step and controls the overall rate of deformation (Renard et al.,

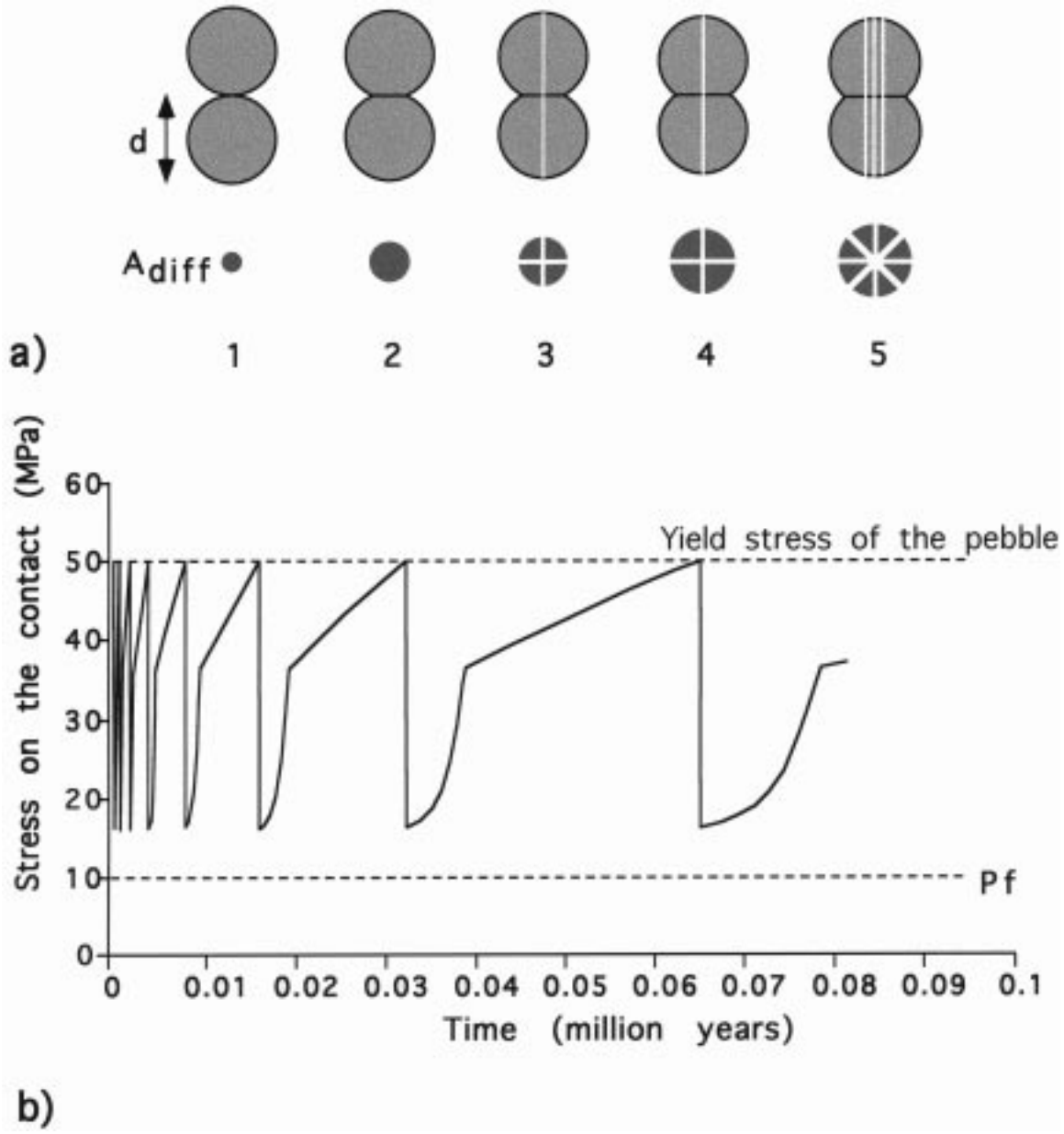

Fig. 3. Pressure solution on two spherical pebbles (or grains) with progressive deformation at constant indentation-rate. It is assumed that fractures develop when the stress on the surface of contact reaches the yield strength of the pebble (or the grains) and cuts the surface of dissolution A_{diff} into two parts. (a) During deformation, the circular contact between the two spherical pebbles increases (step 1 to 2 and step 3 to 4). When fractures occur (step 3 and step 5), each solid–trapped fluid–solid interface is divided by two, consequently the mean distance of slow diffusion is reduced since it is assumed that fractures provide a (relatively) fast path for solute diffusion. (b) Evolution of the normal to the dissolution contact stress values with time. Stress is computed through Eq. (4) where the rate of indentation is constant. The strain rate is fixed to be $10^{-14}\,s^{-1}$. The initial diameter of each pebble, d, is 10 cm. The upper limit is the yield stress of a limestone (50 MPa). Physico-chemical conditions correspond to a depth of 1 km (T = 303 K and P_{pore} = 10 MPa). Molar volume of calcium is 37 cm^3/mol. The concentration of calcium in the free pore fluid is 1.4×10^{-4} mol/l. The concentration of calcium is greater in the contact due to the effect of stress on the chemical potential of carbonate. The coefficient of diffusion along the contact is taken to be an order of magnitude less than for diffusion in bulk water. The water-film thickness exponentially decreases with stress down to a minimum value of 0.5 nm at 26 MPa of effective stress. The non-linear stress vs time relation is due to the non-linear relations between stress, solubility and water-film thickness (see text).

1997). Thus, the rate of indentation of one pebble into another G_{ind} is equal to:

$$G_{ind} = -\frac{2\pi D(T)w(P_{cont}(\text{time}) - P_f)[c_{cont}(P_{cont},T,\text{time}) - c_{pore}(P_f,T)]V_{calc}}{A_{diff}(\text{time})} = \text{constant} \quad (4)$$

where w (m), the thickness of the trapped water film, is an exponential function of $(P_{cont} - P_f)$ where P_{cont} is the stress across the contact and P_f the pore fluid pressure (Renard and Ortoleva, 1997). $D(T)$ with units of $m^2\,s^{-1}$ is the temperature-dependent coefficient of diffusion of calcium inside this fluid film. The concentrations of calcium carbonate inside the contact, c_{cont}, and in the pore c_{pore} ($mol\,m^{-3}$) depends on temperature and on the stress inside the contact P_{cont} and the pore pressure P_f (MPa), respectively (Gibbs, 1877; Stumm and Morgan, 1981). V_{calc} is the molar volume of calcium carbonate and A_{diff} (m^2) is the surface area of the contact along which diffusion occurs (Fig. 3a). In the model it is assumed that the rate of indentation G_{ind} is constant and time independent. If the temperature and the pore pressure are known, it is possible to calculate the pressure across the contact, P_{cont}, through Eq. (4). The pebble accommodates the rate of indentation by pressure solution, but, as the surface of contact between the pebbles, A_{diff}, increases with time (Dewers and Ortoleva, 1990; Onasch, 1993), the stress on it, P_{cont}, increases as well (see Eq. 4), until the yield stress of the pebble is reached and fracture occurs. After fracture, for simplification, the geometry and the location of the fractures are chosen such that the surface for diffusion is divided by two. Consequently, pressure solution is more efficient and can accommodate the constant rate of displacement. Therefore, the stress on the contact decreases under the yield stress limit. In the model, it is assumed that, even if fractures partially heal by precipitation of the dissolved material, they stay a favored path for solute diffusion and the coefficient of diffusion of calcium in the fractures is greater than along the pebble interface.

Comments on the stress vs time curve may be summarized as follows. A viscous–brittle cycle can develop through geological times with ductile-pressure solution on long time scales associated with brittle-fracturing on short time scales (Fig. 3b). The constant yield stress associated with fracture is due to the simplicity of the assumptions for fracture development. In natural deformation the process must be much more unstable due to the hazard development and spacing of the fracture network which plays a crucial role in the model. The progressive change of the mean slope of the stress vs time curve with time and the progressive increase of the duration of the cycles are linked. This happens because of the assumption of constant displacement rate occurring on a spherical pebble: for the same thickness of removed species, increase of the contact area is the fastest at the beginning of the process. The non-linear aspect of the curve emerges from the non-linear relationships between stress and water film thickness. Between 0 and 26 MPa deviatoric stress the water film thickness decreases exponentially with stress (Renard and Ortoleva, 1997). Above 26 MPa the water film stays almost constant (around 0.5 nm) and corresponds to a couple of layers of molecules adsorbed within the grain contact. This transition between a decreasing thickness and a constant thickness explains the sudden change of slope at around 36 MPa.

Without fracture the pressure solution strain rate involving an indented pebble (thus increase of the area of dissolution) should progressively decrease down to very low values. The model explains the significant strain-rate values observed for alpine molassic conglomerates: 10^{-14}–$10^{-15}\,s^{-1}$ (McEwen, 1978; Gratier and Gamond, 1990). However, the model is also pertinent for the deformation of non-porous rocks when the dissolution area progressively grows as the solution surface propagates: Cosgrove (1976, solution cleavage), Fletcher and Polard (1981, anticrack model). Due to the strain-rate inverse dependence on the diameter of the surface of dissolution (Eq. 2) most applications of pressure solution laws have been proposed with small distances of mass transfer (i.e. deformation maps of Rutter, 1976, mass transfer at the grain scale: 100 μm). However, stylolites, or solution cleavages, which are very common markers of pressure solution develop in limestones, or in granitic rocks, at millimetric or centimetric scales. In this case it is often observed that fractures develop perpendicular to the solution surfaces in order to reduce the mean distance of mass transfer (Gratier et al., 1993, figs. 3 and 5) and in order to allow the deformation to be accommodated by pressure solution at significant strain rates.

The modeled stress vs time relation including fracture processes in pressure solution laws (Fig. 3b) gives an order of magnitude of the viscosity coefficient for pressure solution creep. The mean stress value needed to maintain the constant strain rate is about 32.5 MPa. Using Eq. (1), $\dot{\varepsilon}$ being equal to $10^{-14}\,s^{-1}$, an approximate value of 3×10^{21} Pa s is found for the pressure solution creep viscosity coefficient. By mechanical modeling at the crustal scale, Nino et al. (1998) found the same order of magnitude for the viscosity of sediments (Ventura basin, California): 10^{20}–10^{21} Pa s.

5. Conclusions

The kinetics of pressure solution creep is inversely proportional to the diameter of the surface of dissolution. When dissolution areas increase during progressive deformation, either the pressure solution strain rate should decrease with time or the stress values should increase in order to maintain significant strain rate.

Both experimental and natural observations show that fracture processes occur during pressure solution creep to regulate this evolution with time. For example, at constant strain rate, pressure solution may be associated with an increase of stress values leading to fracture development. Fractures develop channels perpendicular to the dissolution interface and partition it into small domains of trapped fluid, increasing the pressure solution strain rate.

A numerical model is given which shows this complex interaction between pressure solution and fracturing processes and explains how these two mechanisms are so often associated in natural deformation. At constant displacement rate, a stress vs time cyclic process is calculated. A mean value of viscosity of 3×10^{21} Pa s is derived from the numerical model applied to conglomerate of indented pebbles.

The mechanical behavior of the crust appears to be much more complex than thought before, integrating successive brittle (fast) incremental events and viscous (slow) deformation which are not independent. It is suggested that geologic modeling of the upper crust (creep laws) must integrate this complex mechano-chemical interaction both by developing new modeling concepts and by deriving constitutive equations based on experimental data.

Acknowledgements

We would like to thank A.-M. Boullier, J. Evans and an anonymous reviewer for stimulating discussions and helpful review.

References

Applin, K.R., 1987. The diffusion of dissolved silica in dilute aqueous solution. Geochimica et Cosmochimica Acta 51, 2147–2151.

Atkinson, B.K., 1984. Subcritical crack growth in geological materials. Journal of Geophysical Research 89, 4077–4114.

Cosgrove, J.W., 1976. The formation of crenulation cleavage. Journal of the Geological Society of London 132, 155–178.

Darot, M., Reushlé, T., Gueguen, Y., 1985. Fracture parameters of Fontainebleau sandstones: experimental study using high temperature controlled atmosphere Double Torsion apparatus. In: Ashworth, E (Ed.), Research and Engineering Applications in Rocks Masses. Balkema, Rotterdam, pp. 463–470.

De Bremaecker, J.Cl., 1987. Thrust sheet motion and earthquakes mechanisms. Earth and Planetary Sciences Letters 83, 159–166.

den Brok, S.W.J., 1998. Effect of microcracking on pressure solution strain-rate: The Gratz grain-boundary model. Geology 26, 915–918.

Dewers, T., Ortoleva, P., 1990. A coupled reaction/transport/mechanical model for intergranular pressure solution stylolites, and differential compaction and cementation in clean sandstones. Geochimica et Cosmochimica Acta 54, 1609–1625.

Fletcher, R.C., Polard, D.D., 1981. Anticrack model for pressure solution surface. Geology 9, 419–424.

Gibbs, J.W., 1877. On the equilibrium of heterogeneous substances. Transactions of the Connecticut Academy 3, 108–248 and 343–524.

Gratier, J.P., 1993a. Experimental pressure solution of halite by an indenter technique. Geophysical Research Letters 20, 1647–1650.

Gratier, J.P., 1993b. Le fluage des roches par dissolution–cristallisation sous contrainte dans la croûte supérieure. Bulletin de la Société Géologique de France 164, 267–287.

Gratier, J.P., Gamond, J.F., 1990. Transition between seismic and aseismic deformation in the upper crust. In: Knipe, R.J., Rutter, E.H. (Eds.), Deformation, Mechanisms, Rheology and Tectonics. Geological Society of London Special Publication 54, pp. 461–473.

Gratier, J.P., Chen, T., Hellmann, R., 1993. Pressure solution as a mechanism for crack sealing around faults, natural and experimental evidence. In: Hichkmann, S., Sibson, R., Bruhn, R. (Eds.), Mechanical Involvement of Fluids in Faulting. USGS Open File Report 228, pp. 279–300.

Gratz, A.J., 1991. Solution transfer compaction of quartzites: progress toward a rate law. Geology 19, 901–904.

Houseknecht, D.W., 1988. Intergranular pressure solution in four quartzose sandstones. Journal of Sedimentary Petrology 58, 228–246.

Lehner, F.K., Bataille, J., 1985. Nonequilibrium thermodynamics of pressure solution. Pure and Applied Geophysics 122, 53–85.

McEwen, T.J., 1978. Diffusional mass processes in pitted pebble conglomerates. Contributions to Mineralogy and Petrology 67, 405–415.

Milliken, K.L., 1994. The widespread occurrence of healed microfractures in siliclastic rocks: Evidence from scanned cathodoluminescence imaging. In: Nelson, C.S., Laubach, S.E. (Eds.), Rock Mechanics. Balkema, Rotterdam.

Moretti, I., Baby, P., Mendez, E., Zubieta, D., 1996. Hydrocarbon generation in relation to thrusting in the Sub Andean Zone from 18 to 22°S, Bolivia. Petroleum Geoscience 2, 17–28.

Nino, F., Chery, J., Gratier, J.P., 1998. Mechanical modelling of compressional basins: origin and interaction of faults, erosion and subsidence, in the Ventura basin, California. Tectonics 17, 955–972.

Onasch, C.M., 1990. Microfractures and their role in deformation of a quartz arenite from the central Appalachian foreland. Journal of Structural Geology 12, 883–894.

Onasch, C.M., 1993. Determination of pressure solution shortening in sandstones. Tectonophysics 227, 145–159.

Onasch, C.M., Dunne, W.M., 1993. Variation in quartz arenite deformation mechanisms between sequence and duplexes. Journal of Structural Geology 15, 465–475.

Ortoleva, P.J., 1994. Geochemical Self-Organization. Oxford University Press, New York.

Raj, R., 1982. Creep in polycrystalline aggregates by matter transport through a liquid phase. Journal of Geophysical Research 87, 4731–4739.

Raj, R., Ashby, M.F., 1981. On grain boundary sliding and diffusional creep. Metallurgical Transactions 2, 1113–1128.

Renard, F., Ortoleva, P., 1997. Water film at grain–grain contacts:

Debye–Huckel, osmotic model of stress, salinity and mineralogy dependence. Geochimica et Cosmochimica Acta 61, 1963–1970.

Renard, F., Ortoleva, P., Gratier, J.P., 1997. Pressure solution in sandstones: influence of clays and dependence on temperature and stress. Tectonophysics 280, 257–266.

Rutter, E.H., 1976. The kinetics of rock deformation by pressure solution. Philosophical Transactions of the Royal Society of London 283, 203–219.

Shen, Z.-k., Dong, D., Herring, T., Hudnut, K., Jackson, D., King, R., McClusky, S., Sung, L., 1997. Crustal deformation measured in Southern California. Transactions of the American Geophysical Union 78, 477.

Sorby, H.C., 1865. On impressed limestone pebble. Proceedings West Yorkshire Geological Society 4, 458–461.

Stumm, W., Morgan, J., 1981. Aquatic Chemistry: an Introduction Emphasizing Chemical Equilibria in Natural Waters. Wiley, New York.

Tada, R., Siever, R., 1986. Experimental knife-edge pressure solution of halite. Geochimica et Cosmochimica Acta 50, 29–36.

Tucker, M.E., 1981. Sedimentary Petrology, Geoscience Texts. Blackwell Science, Oxford.

Weyl, P.K., 1959. Pressure solution and the force of crystallization: a phenomenological theory. Journal of Geophysical Research 69, 2001–2025.